Food and Chemical Toxicology 219 (2027) 116492

Contents lists available at ScienceDirect

Food and Chemical Toxicology

journal homepage: www.elsevier.com/locate/foodchemtox

Toxicogenomic studies reveal early mitochondria and ribosome dysfunction in cadmium carcinogenicity

Monica Oldani [a,1], Marco Fabbri [c,1], Pasquale Mechioretto [b], Matilde Forcella [a,*], Paola Fusi [a,d], Chiara Urani [b,d,**]

[a] Department of Biotechnology and Biosciences, University of Milano-Bicocca, Piazza della Scienza 2, 20126, Milan, Italy
[b] Department of Earth and Environmental Sciences, University of Milano-Bicocca, Piazza della Scienza 1, 20126, Milan, Italy
[c] Department of Clinical and Experimental Medicine, University of Insubria, 21100, Varese, Italy
[d] Integrated Models for Prevention and Protection in Environmental and Occupational Health, Interuniversity Research Center (MISTRAL), 25121, Brescia, Italy

ARTICLE INFO

Handling Editor: Professor Matthew Wright

Keywords:
Cadmium
Carcinogenesis
Cell transformation assay
Early markers
Mechanisms
Integrated approach

ABSTRACT

Cadmium (Cd) is a widespread non-essential metal released by natural and anthropogenic activities leading to concern for human health. The main sources of human Cd exposure are food, drinking water and tobacco smoke. Cd enters the cells through a variety of channels and transport pathways mimicking essential ions. Once uptaken, Cd can lead to different diseases, including cancer, although its mechanisms are still not fully elucidated. In this work, we performed a toxicogenomics study based on whole-genome microarray analysis of gene modulation induced by Cd treatment (1 and 2 μM $CdCl_2$) in C3H10T1/2 cells, as a model for *in vitro* carcinogenicity studies in the Cell Transformation Assay. Exploratory analyses using Principal Component Analysis, applying combinations of differential expression analyses using generalized linear models were used. Differentially expressed genes as well as the log(FC) were calculated by limma approach. Downstream analyses, such as Gene Ontology and pathway enrichment analysis, along with weighted co-expression network analyses were performed. Data suggest that in the first 24 h, the upregulation of metallothioneins and glutathione S- transferase (Gstα 1–3) are not fully efficient in preventing damages caused by Cd. Mitochondria and ribosome dysfunction emerge as the main causes of Cd-induced carcinogenesis, as suggested by results.

1. Introduction

Cadmium (Cd) is a heavy metal discovered in 1817 as an impurity of zinc carbonate ($ZnCO_3$) and found at low concentrations in the Earth's crust combined with oxygen (cadmium oxide), chlorine (cadmium chloride), or sulfur (cadmium sulfate, cadmium sulfide). However, the mobilization of Cd in the environment mainly due to anthropogenic activity (batteries, pigments, metal coatings, and plastics), has made this metal a pollutant of high concern. In this regard, it has been shown that Cd can lead to ecosystems destruction, also at much lower doses than most toxic metals (Jaishankar et al., 2014). Furthermore, it has been known that Cd dispersed in the environment can persist in soils and sediments for decades, exacerbating the potential environmental damage (Wuana and Okieimen, 2011). Cd has no nutritional and physiological roles but is a contaminant of almost all food items and is detectable over time in airborne and water mostly in highly anthropic and industrial areas. The principal sources of Cd exposure for the general population are food, tobacco smoke, drinking water, and air. An estimate in a typical Australian diet reports average and high values of 30 and 93.5 μg/day of cadmium (Cirovic et al., 2024). For these reasons, Cd remains a source of concern for human health, especially for populations living in polluted areas. Once absorbed, due to its exceptionally long half-life in the human body (15-35 years), Cd irreversibly accumulates in kidneys, lungs or liver and can induce several diseases, including cancer (Bernard, 2008; Thévenod and Lee, 2013). In this regard, Cd was classified as a human lung carcinogen (Group 1) by the World Health Organization's International Agency for Research on Cancer (IARC) and by the German MAK Commission. However, dietary exposure to this metal and consequent cancer risk to different tissues are underestimated, as evidenced by epidemiological studies and meta-analyses (Cirovic and

* Corresponding author. Department of Biotechnology and Biosciences, University of Milano-Bicocca, Piazza della Scienza 2, 20126, Milan, Italy.
** Corresponding author. Department of Earth and Environmental Sciences, University of Milano-Bicocca, Piazza della Scienza 1, 20126, Milan, Italy.
E-mail addresses: matilde.forcella@unimib.it (M. Forcella), chiara.urani@unimib.it (C. Urani).
[1] These authors contributed equally to this work.

https://doi.org/10.1016/j.fct.2026.116492
Received 9 April 2026; Received in revised form 26 October 2026; Accepted 9 November 2026
Available online 11 November 2026
0278-6915/© 2026 The Authors. Published by Elsevier Ltd. This is an open access article under the CC BY license (http://creativecommons.org/licenses/by/4.0/).

Satarug, 2024).

Based on the literature data, multiple Cd effects on different targets can be highlighted and are reviewed (Peana et al., 2022; Rasin et al., 2025; Yang et al., 2025). Among the effects, at molecular level altered cell proliferation (Asara et al., 2013), tissue injury through oxidative stress increase (Henkler et al., 2010), inhibition or upregulation of transport pathways (Yang and Shu, 2015), modification in the homeostasis of other divalent cation (Zn^{2+} and Ca^{2+}), dysregulation of zinc transporters (Bovio et al., 2026) and inhibition of heme synthesis (Schauder et al., 2010) were observed. In addition, different cell organelles are targets of Cd toxicity, such as mitochondria and the endoplasmic reticulum (ER) (Bovio et al., 2021; Lee and Thévenod, 2020). Following Cd uptake in the cells, some free metal ions or some Cd-metallothionein complexes not only remain in the cytosol but can also penetrate the mitochondria. Subsequently, in these organelles, high concentrations of Cd can lead to altered morphology and dynamics, and to the inhibition of mitochondrial functions either by inhibiting the activity of complexes II and III of the electron transport chain or by inducing the activation of apoptotic signaling (Branca et al., 2020). On the ER, Cd is highly effective in inducing stress, initiated by oxidative stress and lowered calcium. At the molecular level, epigenetic changes, DNA repair mechanisms damage and the telomere shortening are among the features altered by Cd (Lee and Thévenod, 2020; Ryoo et al., 2025; Tan et al., 2023). Cd can alter gene expression (Callegaro et al., 2018; Fabbri et al., 2012; Zhou et al., 2004) acting as a transcriptional regulator for both normal and pathological cell types (Bertin and Averbeck, 2006; Luparello, 2021). Cd intake can upregulate the expression of several genes related to the metal ion stress response and detoxification processes (e.g., those coding for metallothioneins, glutathione and heat shock proteins) or can change the expression of genes connected with inflammation, metabolism, and can lead to the deregulation of transporters and onco- or tumor suppressor genes (Callegaro et al., 2018; Forcella et al., 2022; Koizumi and Yamada, 2003).

As it emerges, several mechanisms are activated or dysregulated by this metal, and many of them are known to contribute to carcinogenesis processes. However, a general picture of the sequence of events triggering and/or contributing to processes involved in carcinogenesis has still to be clearly defined. In this study we performed a whole-genome transcriptomics analysis to deeply explore this complex pathological process at the molecular level and to provide a general picture of events and their possible interplay at early stages. A toxicogenomic approach provides a useful tool to analyze individual genes, specific gene sets and signatures, and gene networks and functional pathways leading to malignant cell transformation and to the comprehension of cross-talk between genotoxic and non-genotoxic mechanisms (Corvi et al., 2017; Liu et al., 2019). As a study model for Cd carcinogenesis, we used the C3H10T1/2 clone 8 mouse embryonic fibroblasts (C3H), one of the recognized cell models for the study *in vitro* of carcinogenicity process (Cell Transformation Assay, CTA). C3H cells were treated with two sub-lethal concentrations of Cd for 24 h (1 and 2 μM). The lowest cadmium concentration was selected since it can induce malignant cell transformation and *foci* (colonies of transformed cells) formation in the *in vitro* CTA, as previously described (Forcella et al., 2016; Urani et al., 2009), thus giving hints on the molecular processes involved in the early carcinogenic steps. The highest concentration was used to investigate the dose-dependent effect of this metal. Thus, the purpose of this research is both to identify early dysregulated genes as markers of Cd-induced carcinogenesis, and to gain a deeper understanding into its molecular mechanisms, in order to allow better assessment of associated risks at environmental and human-relevant concentrations due to the multiple sources of exposures to this metal.

2. Materials and methods

2.1. Cells and culture conditions

C3H10T1/2 clone 8 (C3H) mouse embryonic fibroblasts (ATCC, CCL 226 lot. n. 58078542) is one of the suitable cell models suggested for *in vitro* carcinogenicity studies (OECD, 2007). Indeed, this cell line is extremely sensitive to carcinogenic compounds and undergoes a spontaneous transformation at a very low rate. Cells were cultured at 37 °C in a humidified incubator supplied with 5 % CO_2 in Basal Medium Eagle (BME, Merck KGaA, Darmstadt, Germany) enriched with 10 % heat-inactivated fetal bovine serum (FBS, Euroclone, Milan, Italy), 2 mM glutamine, 10 mM HEPES and 25 μg/mL gentamicin (Merck KGaA, Darmstadt, Germany). Cells were routinely maintained in 100 mm Ø Petri dishes and split when reached 80 % confluence. The cells were stored in cryovials with 10 % DMSO and put in liquid nitrogen for long-term conservation.

2.2. RNA extraction and purification

For RNA extraction, the cells were seeded at a density of 10^6 cells/dish in 100 mm Ø Petri dishes for the treatments. The following day, the cells were exposed to 1 or 2 μM $CdCl_2$ (Cd) in BME for 24 h. The ultrapure water stock solution (1 mM) of $CdCl_2$ (>97 % purity, code number 104784 R, BDH Laboratory, Milan, Italy) was stored at 4 °C. At the end of treatments, the cells were harvested by trypsinization, lysed in 300 μL RLT buffer (Qiagen, Germantown, MD, USA) with 1:100 β-mercaptoethanol and, by passing 5 times through a blunt 20-gauge needle fitted to a syringe, to obtain homogenates. Samples were stored at −80 °C until RNA was purified from cell samples (controls and Cd-treated) using the RNeasy Plus kit (Qiagen, Germantown, MD, USA). All RNA samples were quantified using a ND-1000 UV-Vis Spectrophotometer (NanoDrop Technologies) and the 260/280 ratio was checked for all samples (above 1.9). The RNA integrity was assessed with the Agilent 2100 Bioanalyzer (Agilent, Santa Clara, CA, USA) and RNA Integrity Number (RIN) was measured above 9.0 for all samples. All these steps have been carried out according to the manufacturer's instructions.

2.3. Microarray expression profiling

All steps required for microarray experiments were performed following the manufacturer's specifications. In brief, Cy3-labeled cRNA was obtained from 500 ng input total RNA using Quick Amp Labeling Kit, One-color (Agilent, Santa Clara, CA, USA). A 1.65 μg cRNA from each labelling reaction (specific activity above 9.0) was hybridized using the Gene Expression Hybridization Kit (Agilent) to the SurePrint G3 Mouse GE 8 × 60K Microarray (G4852, Agilent, Santa Clara, CA, USA), which is an 8 x 60k 60mer slide format. After hybridization, the slides were washed and then scanned with the Agilent G2565BA Microarray Scanner (Agilent, Santa Clara, CA, USA). Three independent replicates were carried out for each treatment and control. The fluorescence intensities on scanned images were extracted and preprocessed by Agilent Feature Extraction Software (v10.5.1.1). Quality control and array normalization was performed in the R statistical environment using the Agi4x44PreProcess package downloaded from the Bioconductor web site (Gentleman et al., 2004). After that, all duplicated genes were eliminated using the function collapseRows of the WGCNA package (Langfelder and Horvath, 2008). The function allows to collapse the rows of the processed matrix, forming a representative row for each group of rows that have the same name. As a result, a sub-matrix of about 22.000 genes was obtained.

2.4. Biostatistical and bioinformatic analyses

We carried out a first data exploration using Principal Component Analysis (PCA) with the built-in R function prcomp. This allowed us to

verify that the groups of interest were sufficiently separated to perform differential expression analyses (DEA). We used the linear model implemented in the Limma R/Bioconductor package (Ritchie et al., 2015) for DEA. We considered as significant the differentially expressed genes (DEGs) with a Log Fold Change (LogFC) ≥ 1 (up-regulated) or ≤ -1 (down-regulated), and with a false discovery rate (FDR) < 0.05 (Smyth, 2004). The analysis was based on the investigation of three different pairwise comparisons: 1 μM Cd versus control (1vsC), 2 μM Cd versus control (2vsC) and 2 μM Cd versus 1 μM Cd (2vs1). We estimated the intersections between the up- and down-regulated genes in the three different comparisons using the Venn diagrams package in R. To determine the functions and the interlinkages of the DEGs, pathway enrichment analyses (KEGG and Gene Ontology) were performed using ShinyGO 0.76.3, an online tool based on several R/Bioconductor packages, and a large annotation of pathway database gathered from many sources for DEA (Ge et al., 2020). Gene Ontology (GO) enrichment analysis was performed on the list of differentially expressed genes using the reference annotation database. Genes associated with GO terms were included in the functional classification. Some entries correspond to transcript identifiers rather than standard gene symbols; however, these transcripts are linked to GO annotations in the database used for the analysis.

To better understand the distribution of DEGs in the different pathways, we applied the R package UpSetR on each category of GO (Conway et al., 2017).

2.5. SDS-PAGE and Western blotting

C3H cells were seeded at a density of 1.5×10^6 cells/100 mm dish and, 24 h after seeding, were treated with 1 μM and 2 μM $CdCl_2$ for 24 h, while untreated cells represented the control. After treatment, the cells were rinsed with ice-cold PBS (10 mM K_2HPO_4, 150 mM NaCl, pH 7.2) and lysed in RIPA buffer (Tris-HCl 50 mM, NaCl 150 mM, NP40 1 %, SDS 0.1 %, sodium deoxycholate 0.5 %, pH 7.5) containing 1 μM leupeptin, 2 μg/mL aprotinin, 1 μg/mL pepstatin and 1 mM PMSF. After lysis on ice, homogenates were obtained by passing 5 times through a blunt 20-gauge needle fitted to a syringe, then a centrifugation was performed at 14000 × g for 30 min at 4 °C. Supernatants were quantified by the BCA protein assay (Smith et al., 1985). To evaluate RPL13A expression level, 60 μg of protein samples were separated on 15 % acrylamide/bisacrylamide gel and then blotted onto a nitrocellulose membrane (Millipore, Burlington, MA, USA). SDS-PAGE and Western blot were performed by standard procedures (Laemmli, 1970), and the following primary antibody had been used: anti-RPL13A (dilution 1:1000, #PA549192 Life Technologies Italia, Milan, Italy), anti-MRPL14 (dilution 1:1000, #PA551008 Life Technologies Italia, Milan, Italy) with anti-α-tubulin (dilution 1:2000, #T6199 Merck KGaA, Darmstadt, Germany) as loading control. Anti-mouse IgG HRP-conjugated secondary antibodies (dilution 1:8000, #7076 Cell Signaling Technology, Danvers, MA, USA) and anti-rabbit IgG HRP-conjugated secondary antibodies (dilution 1:5000, #7074 Cell Signaling Technology, Danvers, MA, USA) were used as secondary antibody and proteins were visualized using ECL detection system (EuroClone, Milan, Italy), according to the manufacturer's instructions. Protein levels were quantified by densitometric analysis of immunoblots using ImageJ software (National Institute of Health, USA). All other chemicals were purchased from Merck KGaA, Darmstadt, Germany.

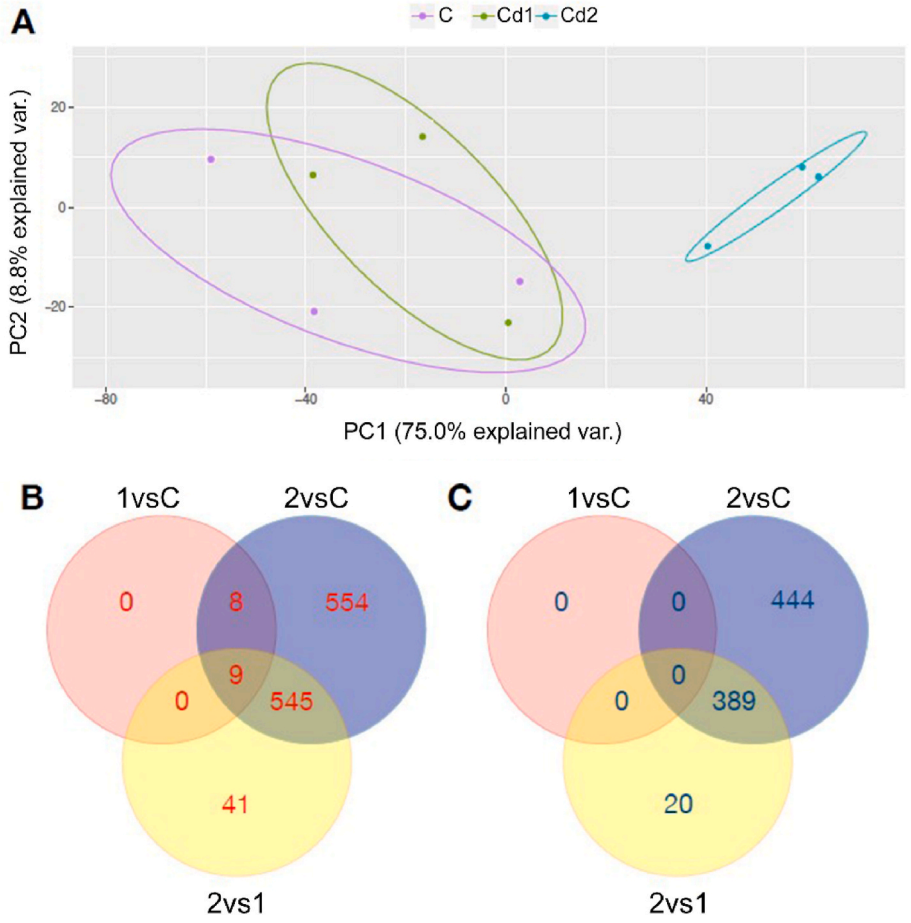


Fig. 1. Genes expression profiles upon Cd exposure: Principal Component Analysis (A) and Venn Diagrams (B and C). In B, the Venn Diagram represents the number of the up-regulated genes following Cd exposure; in C, the Venn Diagram represents the down-regulated genes.

3. Results

3.1. Cadmium induces a dose-dependent response on gene expression

Results from principal component analysis (PCA) on gene expression data are reported in Fig. 1A. The first principal component (PC1) explained 75 % of the samples' variance, while the second principal component (PC2) accounted for 8.8 %. Based on these two PCs, the distribution of our three experimental data groups (Control, 1 μM Cd, and 2 μM Cd) showed that the maximal amount of variance arises when cells were treated with 2 μM Cd. Indeed, 1 μM Cd treated cells and the control group showed a high overlap in the PCA space, while 2 μM $CdCl_2$ treated cells were outliers, compared to the other two groups. Therefore, a 24 h treatment with 2 μM $CdCl_2$ is sufficient to radically change the gene expression profiles of C3H cells.

Subsequently, we performed a deeper analysis of transcriptomic data using a statistical framework for differential expression analysis (DEA) (Ritchie et al., 2015) to better evidence the differentially expressed genes (DEGs). In particular, we took into consideration three pairwise comparisons: 1 and 2 μM $CdCl_2$ each versus control (1vsC and 2vsC) and 2 μM $CdCl_2$ versus 1 μM $CdCl_2$ (2vs1). The Venn diagrams in Fig. 1B and C represent a summary of the DEA calculations. The diagram in Fig. 1B illustrates 17 up-regulated genes after treatment with 1 μM $CdCl_2$ (1vsC). Of these, 9 genes were up-regulated in all the conditions (1vsC, 2vsC, and 2vs1) and 8 common genes were shared between the first and the second comparison (1vsC and 2vsC). No down-regulated genes were observed after 1 μM $CdCl_2$ exposure (Fig. 1C). On the other hand, about 2000 DEGs were evidenced by increasing $CdCl_2$ concentration from 1 to 2 μM. A high number of deregulated genes, namely 554 up- and 389 down-regulated genes, characterized the intersection between 2vsC and 2vs1 respectively. In the 2vsC comparison 554 up-regulated and 444 down-regulated genes were exclusively differentiated (Fig. 1B and C). At least 41 up- and 20 down-regulated genes were distinctive in the third comparison 2vs1 (Fig. 1B and C).

Data for both plots are based on the SurePrint G3 Mouse GE 8 × 60K Microarray experiments normalized using the Agi4x44PreProcess package. A PCA was performed on all genes of the data set to summarize the hidden trends of the transcriptomics data by fitting the whole matrix to orthogonal axes. Purple circle: control; green circle: 1 μM Cd; blue circle: 2 μM Cd. B and C Venn Diagrams used to obtain an effective representation of DEGs in samples treated for 24 h with different $CdCl_2$ concentrations, where 1vsC: 1 μM Cd vs control, 2vsC: 2 μM Cd vs control and 2vs1: 2 μM Cd vs 1 μM Cd. The number of genes shared between different samples is shown in the overlapping regions of the diagram. In both diagrams, the pairwise comparison 1vsC, 2vsC, and 2vs1 are evidenced in salmon, blue, and yellow, respectively.

3.2. Cadmium modulates genes related to metastasis

Investigating the identity of the 17 up-regulated genes observed in the comparison 1 μM $CdCl_2$ vs control (1vsC), we recognized the same genes annotated by (Callegaro et al., 2018) after 24 h of treatment with 1 μM $CdCl_2$ (Table 1). However, we additionally found five other upregulated genes. We identified *LOC625953*, a predictive gene similar

Table 1
List of DEGs obtained in the first (1 μM $CdCl_2$) and second comparison (2 μM $CdCl_2$) compared to C3H control cells (1vsC and 2vsC). The list of the up-regulated genes shows all the 17 up-regulated genes obtained analyzing 1vsC comparison and their trend in 2vsC comparison. Yellow cells in 2vsC group represent the top 10-up-regulated genes in 2vsC. The list of the top 10 down-regulated genes is only reported for the 2vsC comparison, because no down-regulated genes were observed in the 1vsC comparison.

			1vsC			2vsC		
	Gene Description	**Gene Symbol**	**logFC**	**P.Value**	**adj.P.Val**	**logFC**	**P.value**	**Adj.P.Val**
UP	Metallothionein 2	Mt2	4,97	1,26E-12	2,77E-08	4,70	2,27E-12	4,98E-08
	Phosphatidylinositol-4-Phosphate 5-Kinase Type 1 Alpha	Pip5k1a	4,51	5,08E-12	4,97E-08	4,25	9,36E-12	6,84E-08
	Metallothionein 1	Mt1	4,16	6,80E-12	4,97E-08	4,08	8,33E-12	6,84E-08
	/	chr9:78107225-78118850_F	3,29	1,25E-08	3,63E-05	5,13	1,35E-10	2,96E-07
	Glutathione S-Transferase Alpha 1	Gsta1	3,25	6,36E-09	2,79E-05	5,03	7,41E-11	2,71E-07
	Prolactin family 2, subfamily c, member 5	Prl2c5	3,20	3,64E-07	0,00061335	4,90	5,23E-09	6,37E-06
	Glutathione S-Transferase Alpha 2	Gsta2	3,18	1,49E-08	3,63E-05	5,23	9,31E-11	2,88E-07
	/	chr9:78104935-78116974_F	3,18	1,42E-08	3,63E-05	5,14	1,05E-10	2,88E-07
	Predicted to have glutathione transferase activity.	Gm10639	2,61	1,39E-08	3,63E-05	4,61	4,14E-11	1,81E-07
	/	chr11:18367482-18393258_R	2,36	2,12E-09	1,16E-05	3,12	1,23E-10	2,96E-07
	Predictive gene similar to GST class-alpha coding gene	LOC625953	2,25	1,90E-08	4,16E-05	4,21	3,11E-11	1,70E-07
	Growth Differentiation Factor 15	Gdf15	2,09	7,08E-08	0,00012939	3,21	9,41E-10	1,59E-06
	C-C Motif Chemokine Receptor 8	Ccr8	2,05	5,90E-08	0,00011751	2,15	3,80E-08	3,08E-05
	Glutathione S-Transferase Alpha 3	Gsta3	1,82	7,67E-07	0,00112107	3,70	6,21E-10	1,13E-06
	Solute Carrier Family 30 Member 1	Slc30a1	1,56	1,02E-06	0,00139219	1,23	9,40E-06	0,0010805
	Aldolase, Fructose-Bisphosphate C	Aldoc	1,55	4,65E-07	0,00072839	1,79	1,08E-07	6,33E-05
	Carboxylesterase 5A	Ces5	1,12	3,64E-06	0,00419421	1,77	4,31E-08	3,37E-05
DOWN	Collagen type V alpha 1 chain	Col5a1				-2,06	3,21E-05	0,00159192
	/	chr10:94900849-94928059_R				-2,05	1,10E-05	0,00115002
	Collagen type II alpha 1 chain	Col2a1				-2,04	0,00010281	0,00224842
	Collagen type I alpha 1 chain	Col1a1				-1,96	1,29E-06	0,00036295
	Collagen type I alpha 2 chain	Col1a2				-1,95	0,0007014	0,00504819
	Pre-MRNA Processing Factor 8	Prpf8				-1,93	9,97E-05	0,00222454
	Golgi Glycoprotein 1	Glg1				-1,90	0,00011129	0,00232536
	Fibronectin 1	Fn1				-1,89	0,00013489	0,00247828
	ADAM Metallopeptidase With Thrombospondin Type 1 Motif 15	Adamts15				-1,85	4,91E-07	0,00017943
	Fibrillin 2	Fbn2				-1,85	0,00016178	0,00266822

to the *Glutathione S-transferase Ya chain* (*GST class-alpha*) coding gene, the *Carboxylesterase 5A* (*Ces5*) coding gene, responsible for the hydrolysis of various xenobiotics, and three genes not yet classified. The complete list of the DEGs with their respective Log fold change (LogFC) is shown in Table 1. In the same table, given the high amount of DEGs in 2 μM Cd vs control (2vsC) comparison, we decided to highlight the top 10 up- and down-regulated genes obtained after the treatment with 2 μM Cd. The results of the 1vsC comparison match those obtained in the 2vsC comparison (Table 1, yellow cells). In contrast, down-regulated genes were only observed when we treated the cells with 2 μM $CdCl_2$ (Table 1). Among the top 10 down-regulated genes in the 2vsC comparison, we found four genes belonging to the family of proteins that provides instructions for producing collagen: *Collagen type* (*Col*) *5a1*, *Col2a1*, *Col1a1*, and *Col1a2*, while other genes, coding for extracellular matrix (ECM) proteins like *Fibronectin 1* (*Fn1*), *Fibrillin 2* (*Fbn2*), *ADAM Metallopeptidase* and *Thrombospondin Type 1 Motif 15* (*Adamts15*) were found to be down-regulated.

Finally, we investigated the trend of all the 17 up-regulated genes acquired in the 1vsC comparison (Fig. 2). It should be noted that, although all these genes were up-regulated both in the 1vsC and the 2vsC comparisons, in the second comparison most of these genes showed an increase in their logFC, suggesting a dose-dependent effect of cadmium. The only exceptions to this trend were those of *MTs* (coding for metallothioneins), *Pip5k1a* (coding for proteins involved in focal adhesion assembly and ruffle assembly), *Ccr8* (coding for a chemokin receptor family member) and *Slc30a1* (coding for proteins that enable calcium channel inhibiting activity and zinc ion transmembrane transporter activity), which showed a similar logFC in both comparisons (Fig. 2).

3.3. Cadmium alters genes related to mitochondria and ribosomes functions

To delineate the cellular response to cadmium exposure, Gene Ontology (GO) enrichment analysis was performed on DEGs. Because the 1vsC comparison yielded only 17 DEGs, which were individually examined above, functional enrichment was not expected to provide additional biologically relevant information. Consequently, downstream GO analyses were restricted to the 2vsC condition. Enrichment analysis of up-regulated genes (Fig. 3) revealed a coherent transcriptional program dominated by translation-related pathways and mitochondrial organization, indicative of early activation of an anabolic and bioenergetic adaptive response (Fig. 3A). UpSet analysis identified 39 genes shared across five highly interconnected Biological Processes: Cellular amide metabolic process, Peptide metabolic process, Amide biosynthetic process, Peptide biosynthetic process, and Translation (Fig. 3D; Supplementary Table S1). The breadth of this intersection supports coordinated up-regulation of both cytoplasmic and mitochondrial translational machinery rather than isolated pathway activation, although to a different extent. In fact cytoplasmic ribosomal protein showed the highest LogFC values, ranging from 0.53 to 0.35, while the expression of mitochondrial ribosomal proteins showed lower LogFC values, ranging from 0.44 to 0.25 (see Supplementary Tables). Notably, a substantial proportion of these 39 genes encodes ribosomal proteins from both compartments. Cytosolic ribosomal components included members of the RPL (Large subunit) and RPS (Small subunit) families (e.g., RPS27L, RPL13A, RPL9, RPS27A, RPS24, RPL34, RPL17, RPL12, RPL35A), while mitochondrial ribosomal proteins comprised MRPL14, MRPL53, MRPL33, MRPL9, MRPS28, MRPL49 and MRPS11. Accordingly, as shown in Fig. 4, Western blotting confirmed the upregulation of RPL13A following $CdCl_2$ administration, with a twofold significant increase in protein level upon treatment with 2 μM $CdCl_2$. The increasing trend of RPL13A is also observed following 1 μM $CdCl_2$ addition, although not significant. On the other hand, the expression of mitochondrial ribosomal protein MRPL14 was not increased upon treatment with cadmium (data not shown).

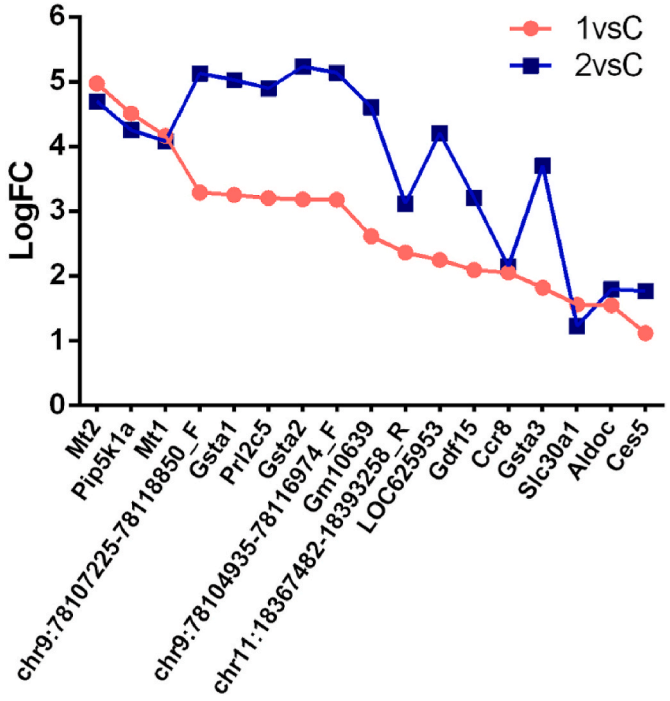


Fig. 2. Plot of logFC (on y-axis) of the 17 up-regulated genes expressed both in the first and the second comparison (1vsC and 2vsC) (see Table 1).

Concomitantly, a distinct 10-gene intersection linking mitochondrial organization and mitochondrial respiratory chain complex assembly (*COX16*, *COX17*, *NDUFB2*, *NDUFB4*, *NDUFB6*, *NDUFS4*, *SDHAF2*, *SLC25A33*, *TMEM126B*, *UQCR10*) indicates transcriptional reinforcement of oxidative phosphorylation components (Fig. 3D; Supplementary Table S1), suggesting that cadmium exposure triggers structural and functional remodeling of the electron transport chain. Cellular Component enrichment further substantiated a pronounced mitochondrial signature (Fig. 3B). A number of 17 genes simultaneously mapped to mitochondrial protein complex, inner mitochondrial membrane, and organelle inner membrane categories (e.g., *NDUFB2*, *NDUFS4*, *TIMM10*, *UQCR10*) (Fig. 3B–E; Supplementary Table S2), supporting a coordinated inner membrane reorganization. Among the 28 genes associated with mitochondrion organization, up-regulation of mitochondrial protein import machinery components, including *TIMM10*, *TIMM8A1*, *TOMM20*, and *TOMM5*, suggests increased protein translocation into mitochondria, consistent with enhanced organelle biogenesis and respiratory complex assembly. Given that cadmium is a potent inducer of mitochondrial reactive oxygen species (ROS), we next examined redox-related processes. In line with oxidative stress activation, genes involved in glutathione metabolism and redox homeostasis were significantly up-regulated. A 7-gene intersection connected peptide/amide metabolism with the glutathione metabolic process (*CHAC2*, *GPX4*, *GSTA1*, *GSTA2*, *GSTA3*, *GSTA4*, *MGST1*), indicating integration of biosynthetic and detoxification pathways. Induction of multiple glutathione S-transferases (*GSTA1–4*) and microsomal GSTs (*MGST1*, *MGST2*) supports enhanced conjugation of electrophilic intermediates and lipid peroxides, whereas up-regulation of *GPX4*, gene coding for a protein localized in mitochondrial membranes, suggests protection against lipid peroxidation within mitochondrial compartments. Increased *GCLM* expression is consistent with stimulated glutathione biosynthesis, while *CHAC2* up-regulation may reflect dynamic glutathione turnover under sustained stress. Furthermore, enrichment of heme and porphyrin catabolic processes (*BLVRA*, *BLVRB*, *HMOX1* gene expression) indicates activation of the heme degradation pathway, a canonical component of oxidative stress adaptation and redox buffering. Collectively, the convergence of Biological Process and Cellular Component enrichment profiles supports

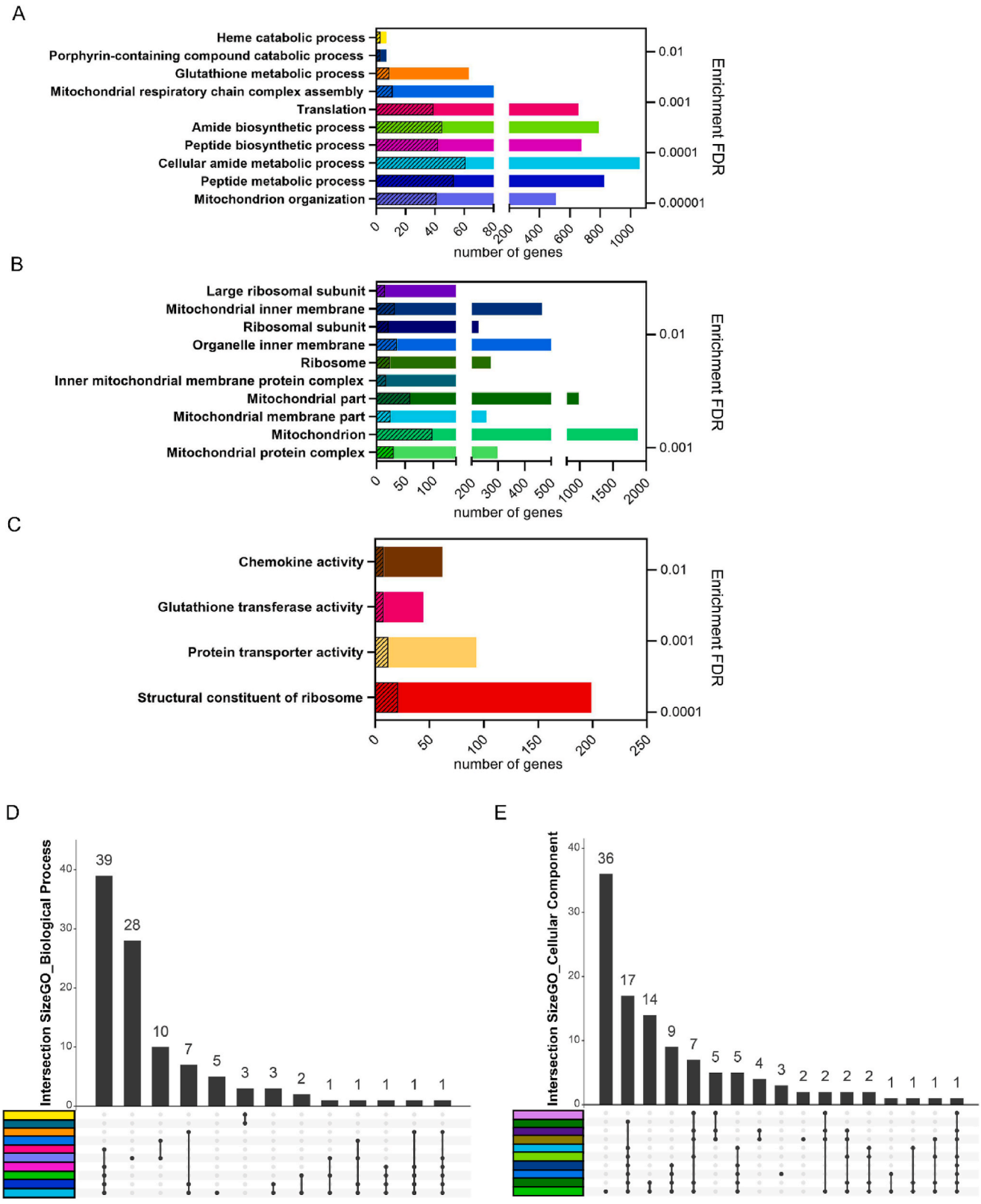


Fig. 3. Classification of the up-regulated genes of the 2vsC comparison in SHINYgo pathway classification. Gene Ontology (GO) enrichment analysis of annotated genes based on their involvement in (A) Biological processes, (B) Localization in a particular cellular compartment, or (C) Molecular functions. The solid color bars indicate the number of DEGs in each pathway, while the background bars indicate the total number of genes that make up that pathway. The statistical significance is represented by Enrichment FDR value: the most significant pathway is the last mentioned. D) and E) UpSetR plots show the real distribution of DEGs in GO and common genes with multiple pathways. The colored horizontal bars at the lower left of the panel represent the different pathways listed in A or B, respectively (one color for each pathway). The vertical bars at the top show DEGs number inside the intersection. The dot pattern to the lower right linked with a black line indicates the intersections between the sets, a single gray dot represents an empty set, and a single black dot indicates no intersection with another set.

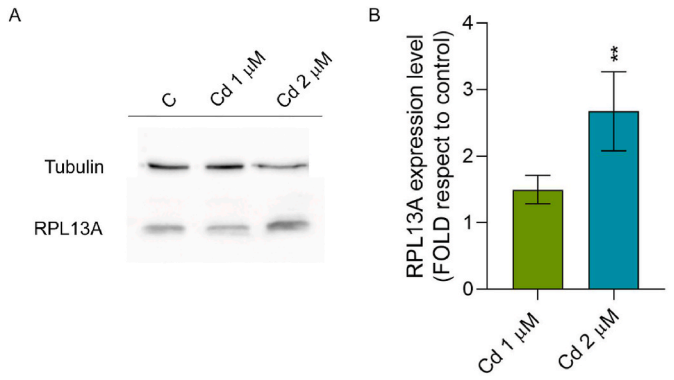


Fig. 4. Western blot analysis on the C3H cell line treated with 1 μM and 2 μM $CdCl_2$ for 24 h. Representative Western blot analysis (A) and densitometric analysis (B) of RPL13A with α-tubulin as loading control. Expression level values are expressed as fold change with respect to the control condition (untreated cells) and each bar indicates the mean ± SEM from at least three biological replicates. Statistical significance from one-way ANOVA with Dunnett's multiple comparison procedure (GraphPad Prism Software version 8.0.2): $^{**}p < 0.01$.

a model of cadmium-induced mitochondrial remodeling characterized by enhanced translational capacity, reinforcement of respiratory chain assembly, and activation of antioxidant defense systems. Rather than representing a nonspecific stress response, these findings delineate a coordinated adaptive transcriptional program aimed at preserving mitochondrial integrity under cadmium-induced oxidative challenge.

3.4. Cadmium inhibits specific gene expression of several biological and molecular processes

GO enrichment analysis of down-regulated transcripts revealed a strong overrepresentation of developmental and morphogenetic processes, with particular convergence on anatomical structure morphogenesis, system development, tissue development, cellular developmental process, and cell differentiation (Fig. 5A). Intersection analysis using UpSetR demonstrated that the most biologically relevant repression module was not confined to single GO categories but spanned multiple developmental lists simultaneously (Fig. 5D). Notably, a core intersection comprising 28 genes shared across all the biological process categories included key regulators of mesenchymal identity and morphogen signaling such as *COL1A1*, *COL2A1*, *COL3A1*, *PDGFRA*, *EGFR*, *mTOR*, *SMAD3*, *SMAD6*, *WNT5A*, *FOXC1*, *SOX9*, *JUN*, *FOXO1* and *EP300* (Fig. 5D–Supplementary Table S3). The coordinated down-regulation of these genes indicates suppression of an integrated morphogenetic transcriptional network controlling extracellular matrix production, growth factor responsiveness, and lineage specification. Additional high-order intersections further reinforced this pattern, revealing coordinated repression of extracellular matrix components (including *COL5A1*, *COL5A2*, *FBN2*, *IGFBP5*), transcriptional regulators (*RELA*, *STAT5A*, *NR2F2*, *KLF2*, *KLF4*), and cytoskeletal or contractile elements such as *ACTA2* (Supplementary Table S3). The Cellular Component analysis provided further mechanistic insights, revealing that not only the extracellular matrix appears to be affected by cadmium treatment, but also the nuclear compartment (Fig. 5B). Indeed, the largest intersection, comprising 184 genes, corresponded to transcripts simultaneously annotated to nucleoplasm, nuclear lumen, nuclear part, and organelle lumen compartments (Fig. 5E). This large nuclear cluster included genes coding for chromatin remodelers (*SMARCA4*, *EP300*, *HDAC4/5/7*, *KDM4B*, *KDM5B*, *KDM6B*, *DNMT3A*, *UHRF1*), for transcription factors (*FOXO1*, *SOX9*, *GLI1*, *GLI3*, *JUN*, *STAT3*, *STAT5A/B*, *NR2F1/2*, *RARA*, *RARG*), and for proliferative regulators such as *MKI67*, *MTOR* and *RPTOR* (Supplementary Table S4). The breadth of this repression indicates that cadmium targets upstream nuclear regulatory architecture, potentially altering chromatin accessibility and transcription factors activity. In parallel, a distinct extracellular matrix cluster emerged, including 28 genes shared between collagen-containing extracellular matrix and extracellular matrix annotations, and 11 genes belonging to collagen trimers and ECM structural components such as *COL1A1*, *COL1A2*, *COL3A1*, *COL4A1*, *COL4A2* and *COL5A1/2* (Fig. 5E–Supplementary Table S4). Molecular Function analysis further supported this interpretation, with enriched GO categories including regulatory region nucleic acid binding and transcription factor binding; moreover, an enrichment of terms related to cation and metal ion binding becomes apparent, consistent with cadmium's known ability to displace zinc from zinc-finger domains and other metal-dependent enzymes (Fig. 5C). In this context, a substantial proportion of the down-regulated genes within the largest intersection (116 genes) in Fig. 5F corresponds to metal ion and cation binding proteins (Supplementary Table S5). Moreover, high-order intersections linked chromatin binding, transcription factor binding, and sequence-specific DNA binding functions, encompassing *EP300*, *SMAD3*, *HDAC4/5*, *JUN*, *SOX9*, *STAT3*, *DNMT3A* and *UHRF1* (Supplementary Table S5). This pattern is consistent with suppression of TGF-β/SMAD signaling, WNT/GLI pathways, nuclear hormone receptor networks, and epigenetic remodeling systems.

3.5. Cadmium upregulates ribosome and mitochondria functions

The pathways in which up and downregulated genes are involved were investigated in detail, through KEGG analysis. Fig. 6A shows all pathways in which the up-regulated genes are involved, while Fig. 6B lists the pathways including the top 10 down-regulated genes. Results show that ribosomes and mitochondrial metabolism are targets of cadmium treatment. In addition, changes at the level of drug metabolism pathways were observed, as well as the upregulation of carcinogenesis pathways. Among the upregulated genes, we found *HMOX1*, *GPx4* and *ADH7* genes that are implicated in the control of ferroptosis. However, *NRF2* and *KEAP1* genes, which are also involved in ferroptosis, were not dysregulated. Interestingly, other up-regulated genes are *HSD11B1*, which is associated with glucocorticoid response during fetal development and *NAT2*, involved in the Chemical carcinogenesis pathway (Fig. 6A). *NAT2* gene is of particular interest since it codes for a protein that can acetylate the amine, hydroxyl, and sulfhydryl groups of many compounds, and its activity can be inhibited by cadmium (Nilusha et al., 2010). Moreover, the down-regulation of genes involved in the PI3K-AKT signaling pathway was observed (*EGFR*, *mTOR*, *AKT1*, *STAT3*, *NF-KB*). The down-regulation of the cyclin D (*CycD*) and *Jun* Proto-Oncogene, AP-1 Transcription Factor Subunit (*c-Jun*) suggests that cadmium blocks cell cycle and t cell survival (Osaki et al., 2004). Indeed, c-Jun is required for the induction of cyclin D and the progression of the cell cycle (Wisdom et al., 1999). Down-regulation of Protein kinase C (PKC), Hexokinase 1 (HK1), and Glycogen Synthase Kinase 3 Beta (GSK3B) suggests an unbalance in the control of glucose homeostasis (Oldani et al., 2021).

4. Discussion

In this work the transcriptomic profile of C3H murine fibroblasts, following 24 h exposure to either 1 or 2 μM $CdCl_2$ (cadmium) is analyzed, with the aim of identifying early markers and mechanistic processes associated with cadmium toxicity and carcinogenicity. The characterization of the effects of such low cadmium concentrations is a key factor in the understanding of cadmium carcinogenicity, which is due to the slow accumulation of this metal in the body. In fact, apart from rare high level cadmium intoxications, like those reported many years ago leading to Itai-Itai disease, a more common situation is a chronic exposure to low cadmium concentrations, through the ingestion of contaminated food and water, polluted air inhalation and cigarette smoke. Due to its very long half-life (15-35 years), cadmium

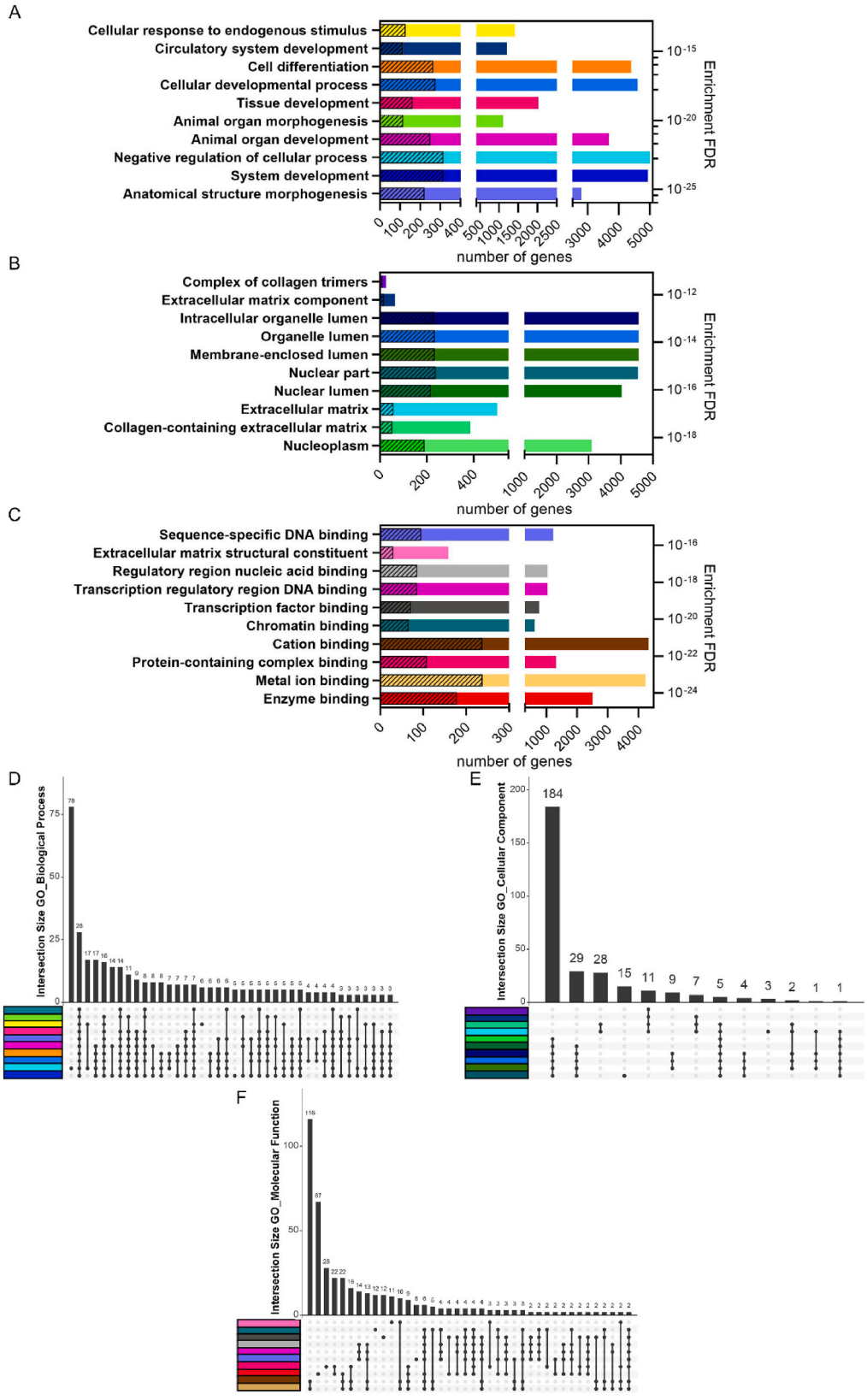


Fig. 5. Classification of the down-regulated genes of the 2vsC comparison in SHINYgo pathway classification. Gene Ontology (GO) enrichment analysis of annotated genes based on their involvement in (A) Biological processes, (B) Localization in a particular cellular compartment, or (C) Molecular functions. The solid color bars indicate the number of DEGs per pathway, while the background bars indicate the total number of genes that make up that pathway. The statistical significance is represented by Enrichment FDR value: the most significant pathway is the last one. D and E) UpSetR plots show the real distribution of DEGs in GO and common genes with multiple pathways. The color horizontal bars at the lower left of the panel represent the different pathways listed in A, B or C, respectively (one color for one pathway). The vertical bars at the top show DEGs number inside the intersection. The dot pattern to the lower right linked with a black line indicates the intersections between the sets, a single gray dot represents an empty set, and a single black dot symbolizes no intersection with another set.

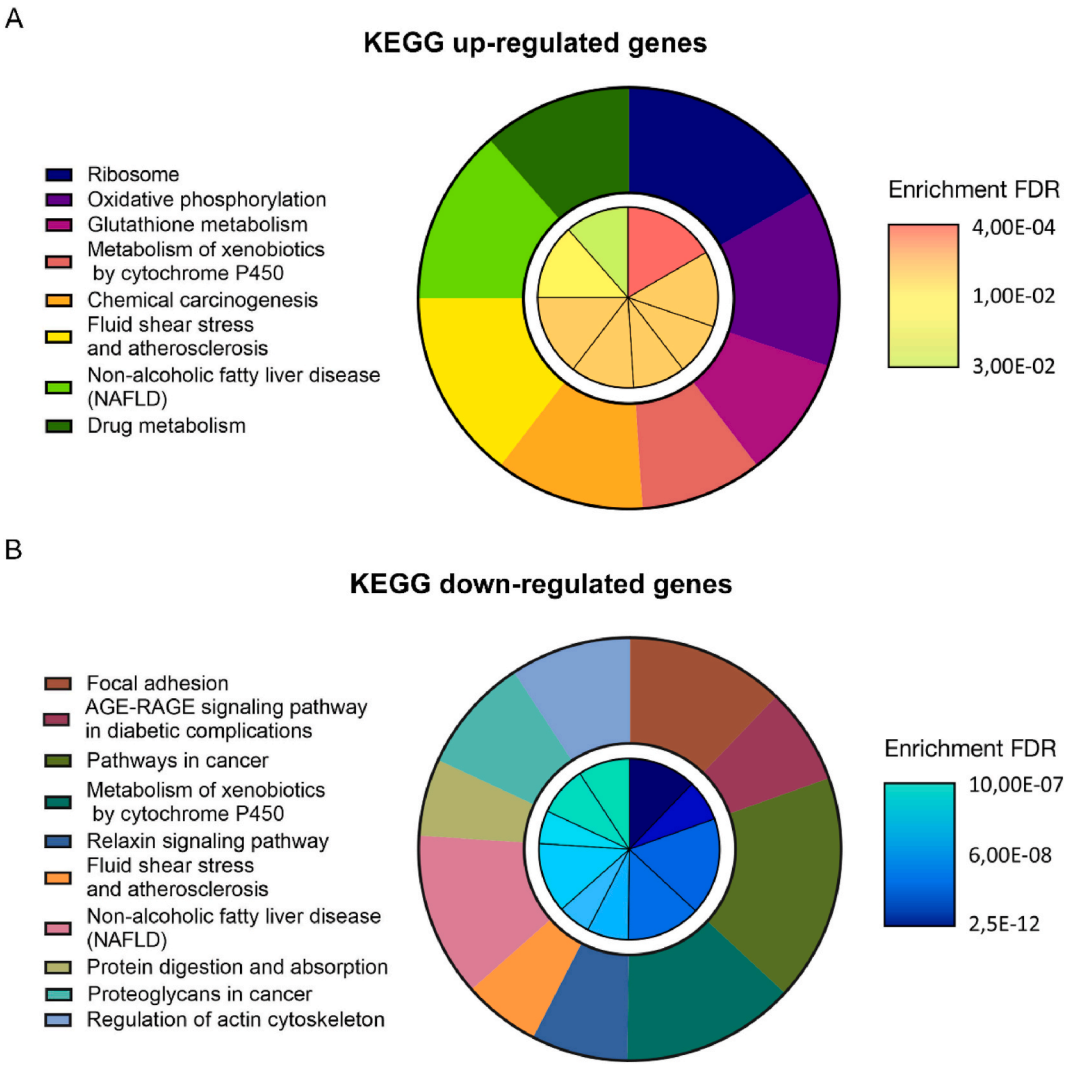


Fig. 6. KEGG analysis. The size of the pie segments represents the number of genes in the pathway of interest. In addition, the outer pie is representative of the number of pathways analyzed, and each color is related to a specific pathway. The colors of the inner pie are representative of the significance connected to each pathway: the darkest color indicates the most significant pathway. A) KEGG up-regulated genes and B) down-regulated genes.

accumulation can easily lead to intracellular concentrations of 1-2 μM, sometimes even reaching 20 μM, as reported in smokers' aorta (Forcella et al., 2020; Mezynska and Brzóska, 2018). Although cells were exposed to low cadmium concentrations, 10 % FBS supplementation was maintained during treatment, in order to avoid introducing other variables beyond cadmium, interfering with cell growth rates. Despite FBS well-known ability to protect from cadmium-induced damage, thanks to its cysteines-rich proteins, in our condition cadmium alterations could be readily detected and showed reproducible dose-dependent effects. The administration of 1 μM $CdCl_2$ for 24 h was chosen because it is the treatment which leads C3H10T1/2 cells to transformation into tumor foci, in the cell transformation assay (CTA) (OECD, 2007); moreover, these conditions were also adopted in a previous work, which allowed to demonstrate that mitochondrial impairment is the main initial metabolic rearrangement induced by cadmium in C3H10T1/2 cells (Oldani et al., 2020b).

The results obtained in this work confirm the early up-regulation of genes involved in the defense against cadmium, like metallothioneins and GST coding genes, balancing oxidative stress, previously reported by our group (Oldani et al., 2020a). However, KEGG analysis additionally showed the involvement of "Chemical carcinogenesis pathways", including other relevant genes, like *NAT2* gene coding for N-acetyltransferase 2, an enzyme responsible for the detoxification of many xenobiotics, and *HMOX1* gene coding for Heme oxygenase 1. Interestingly, the up-regulation of the *HMOX1* was not associated to the dysregulation of other proteins involved in the antioxidant response, such as Nrf2 and Keap1; this is likely related to the dysregulation of iron homeostasis induced by cadmium in different types of cells, as previously reported by our group in SH-SY5Y neuronal cells (Bovio et al., 2026; Forcella et al., 2022), as well as in BV2 microglial cells (Bovio et al., 2024) and in A459 lung cells (Forcella et al., 2022).

The absence of down-regulated genes following 24 h of 1 μM cadmium treatment, previously described (Callegaro et al., 2018) was also confirmed in this work.

The analysis of the comparisons between the two cadmium concentrations used (1vsC and 2vsC) and their respective controls clearly showed a dose-dependent effect of the metal. Cadmium triggers the dysregulation of the expression of about 2000 different genes; of these only 17 are dysregulated by 1 μM cadmium, all the rest are dysregulated by the concentration of 2 μM, showing that cadmium accumulation and persistence in the organisms can lead to severe cellular alterations. Interestingly, among the early events triggered by cadmium is the down-regulation of the genes coding for several extracellular matrix proteins, like collagen, fibronectin and fibrillin coding genes. Collagen has been historically recognized not only as a physical barrier against cancer invasion and tumor cell migration, but also as a significant factor involved

in promoting tumor migration, infiltration, and angiogenesis (Fang et al., 2014; Piao et al., 2021). In addition to the traditional proteolytic ability to degrade extracellular matrix components, members of the ADAMTS family can also exhibit tumor suppressor properties (Dunn et al., 2006; Llamazares et al., 2007; Vázquez et al., 1999; Viloria et al., 2009), and very interestingly *Adamts15* coding gene, recently associated to some tumor-suppressor functions in prostate cancer (Binder et al., 2020), was also found down-regulated in our samples. Therefore, the simultaneous down-regulation of collagen coding genes, *Fibronectin 1* (*Fn1*), *Fibrillin 2* (*Fbn2*), *ADAM Metallopeptidase* and *Thrombospondin Type 1 Motif 15* (*Adamts15*) observed in the 2vsC comparison suggests that cadmium could induce a rearrangement of the extracellular matrix, possibly playing a role in the epithelial-mesenchymal transition (EMT), which is crucial for cancer progression and invasion (Fares et al., 2020). This is well in accordance with previous data obtained in a hepatic cell model (Fabbri et al., 2012), showing that cadmium can alter cell growth, reduce the adhesive properties of cells, and enhance the epithelial-mesenchymal transition (EMT) process. Moreover, the down-regulation of a diverse group of genes coding for cytoskeletal proteins, such as vinculin, actin, actinin, zyxin and filamin, suggests that the cells lose their morphology, prior to losing focal adhesion, as indicated by KEGG analysis. In addition, our data strongly suggest that ECM remodeling precedes and likely facilitates metabolic alterations which are later observed in tumor *foci* of fully transformed cancer cells detected 4-6 weeks after 1 μM cadmium treatment of C3H cells (Forcella et al., 2016). Indeed, it is known that ECM remodeling contributes to developing cancer, not only enhancing the survival and the migration of tumor cells but also developing a pre-malignant microenvironment (Cox and Erler, 2011; Kim, 2026; Levental et al., 2009).

The down-regulation of pre-mRNA processing factor 8 (PRPF8), a core component of the spliceosome and an essential mediator in hypoxia-induced mitophagy, can explain the defects in mitophagy, but not in autophagy previously observed in cadmium treated C3H cells (Oldani et al., 2020b). In fact, neither HIF-1 nor PINK1 proteins were detected in immunochemical analysis after 2 μM cadmium treatment (data not shown). Moreover, PRPF8 knockdown has been shown to dramatically inhibit mitochondrial proteins TOMM20 and TIMM23 degradation, inhibiting hypoxia response and possibly leading to several diseases including neurodegenerative diseases, metabolic diseases, and other aging-related diseases (Xu et al., 2018). The function of *Golgi Glycoprotein 1* (*GLG1*) gene, coding for a protein located in Golgi cisterns and binding fibroblast growth factor and E-selectin, is still to be elucidated (Orth et al., 2020).

The up-regulation of ribosomal functions, observed in our experiments, suggests that either ribosomes are a direct target for cadmium carcinogenicity during short-term metal exposure, or that one of the early adaptive mechanism of cells against cadmium toxicity is a faster and more efficient synthesis of proteins to counteract the inhibitory/destabilizing effects of this metal on many proteins, namely zinc proteins. Very recently, Fuentes and coworkers (Fuentes et al., 2024) proposed a role of ribosomal proteins in cancer in which an aberrant biogenesis and an abnormal ribosome function contribute to the process of carcinogenesis, leading to the new theory of “onco-ribosomes”. Very interestingly, an up-regulation of a cytosolic ribosomal protein (RPL13A) was observed in our samples treated with cadmium, thus suggesting a possible role played by these proteins in the mechanism of carcinogenesis to be further explored.

Cadmium's ability to substitute zinc in several zinc proteins and to affect the Zn proteome in general is well-known (Petering, 2017); this leads to protein function and enzyme activity impairment, as well as increasing their turn-over rate. Moreover, considering Cd and Zn position in the periodic table, respective ions display similar chemical properties: both bind to sulfur ligands with Cd displaying a stronger affinity for thiolate binding than Zn thus interfering with catalysis, as well as disulfide bridges formation during protein folding (Peana et al., 2022; Petering, 2017).

Our data show that mitochondrial functionality is also altered by 1 μM Cd administration. Several genes coding for electron transport complexes subunits were found to be up-regulated, resulting in an enhancement of oxidative phosphorylation, as shown by KEGG analysis; this is well in accordance with previous data from our group, showing an initial upregulation of oxygen consumption rate, maximum respiration rate and spare respiratory capacity, following 24 h treatment of C3H cells with cadmium (Oldani et al., 2020b).

Interestingly, the expression of several genes coding for proteins of the translocase of the outer mitochondrial membrane (TOM) or the translocase of the inner mitochondrial membrane (TIM) was also increased following 1 μM $CdCl_2$ administration. These complexes allow nuclear-encoded mitochondrial proteins synthesized in cytosolic ribosomes, such as most electron transport complexes subunits, to be imported into mitochondria. In particular, TOMM20 and TOMM5 are essential receptors able to select their own interacting partners. TOMM5 is involved in the acid chain hypothesis and in the transfer of preproteins from TOMM22 to TOMM40 channel (Kato and Mihara, 2008; Pitt and Buchanan, 2021); while TOMM20, although it shows an overlapping interactome with TOMM70, has an independent role in the control of infection and pathogenicity and in recognizing the precursors destined for both inner and outer membrane (Komiya et al., 1998; Pitt and Buchanan, 2021). The up-regulation of these proteins could be strictly related to the need to increase mitochondrial import of new electron transfer complexes subunits to replace those damaged by the interaction with cadmium ions. Interestingly, all up-regulated electron transport subunits are imported from the cytosol and accordingly cytosolic ribosomal proteins expression was found upregulated, with the highest LogFC values, ranging from 0.53 to 0.35. The expression of mitochondrial ribosomal proteins showed lower LogFC values, ranging from 0.44 to 0.25 (see Supplementary Tables); in accordance, Western blotting confirmed overexpression of RPL13A, but failed to detect overexpression of mitochondrial MRPL14. These data are also well in accordance with the increase in oxidative phosphorylation previously measured though Seahorse technology, in C3H cells treated for 24 h with 1 and 4 μM $CdCl_2$ (Oldani et al., 2020b).

Moreover, this early response to cadmium toxicity is likely related to the mitochondrial impairment observed in cancer *foci*, developed by C3H cells a few weeks after a 24 h treatment with 1 μM $CdCl_2$, and closely resembles the metabolic rearrangements previously described for one of the isolated and analyzed *foci* (Oldani et al., 2021).

Another interesting, upregulated gene is *HSD11B1*, which is associated with the glucocorticoid response during fetal development and confirms that cadmium is an endocrine disruptor (Ronco et al., 2010).

Interestingly, the PI3K/Akt pathway was found down-regulated in KEGG analysis, suggesting, together with *CycD* gene down-regulation, that cadmium promotes cell cycle arrest, rather than cell proliferation. However, cadmium is a well-known carcinogen and previous experiments, performed in our lab, have shown that 1 μM $CdCl_2$ administration for 24 h, followed by 4-6 weeks recovery without cadmium, can induce the transformation of healthy C3H fibroblasts into fully transformed cancer *foci* (Forcella et al., 2016). Two different kinds of *foci* have been isolated and characterized, showing different metabolic rearrangements: F1 *focus* showing KRAS and ERK activation leading to cell proliferation, and F3 focus showing the activation of PI3K/AKT pathway, leading to increased cell survival (Forcella et al., 2016). This clearly shows that the ECM alteration, promoted by cadmium, is an early event in carcinogenesis, likely inhibiting focal adhesion and promoting a change in cell shape toward a rounder shape. Interestingly, the dramatic change in cell shape and cytoskeletal proteins rearrangement leading to a round shape has been demonstrated to be essential for cancer cells to be able to divide efficiently (Ramkumar and Baum, 2016).

An additional relevant aspect to be discussed, still to be fully understood, is the possible role of epigenetic mechanisms. These dynamic and heritable chromatin alterations, without any modifications in the

genomic sequence, emerged as possible players in cadmium-induced carcinogenesis. Several studies have described cancer cells showing extensive "epigenomic landscape" aberrations driving dysregulation of gene expression profiles (Zhao et al., 2022). Among these, the DNA hypermethylation in gene promoter regions, leading to long-term transcriptional silencing, has been associated with long-term cadmium exposure, while histone modifications and noncoding RNA (lnc RNA and miRNA) affect gene expression contributing to disease progression especially in cancer (Qu and Zheng, 2024).

The ability of cadmium to displace zinc in zinc-finger regions of key proteins and transcription factors, leading to change in conformation and function, is an additional mechanism that might contribute to carcinogenesis (Zhu and Costa, 2020). Based on the same chemical and physical properties, cadmium possibly displaces Fenton-type metals from their binding sites leading to the generation of ROS by the displaced redox-active metal (Zhu and Costa, 2020).

On the whole, our data show that the administration of 2 μM $CdCl_2$ is readily counterbalanced by an anti-xenobiotic, antioxidant response, which cannot prevent extracellular matrix alterations; although no signs of carcinogenesis are observed within the 24 h of cadmium administration, we can speculate that ECM alterations commit some cells to follow the path leading to cancer transformation. These are the cells which will give rise in the following 4-6 weeks, even in the absence of cadmium and following all morpho-functional alterations, to fully transformed cells leading to the formation of tumor *foci*.

Data obtained in this work is part of a broad project for the characterization of the carcinogenesis process induced by cadmium and the improvement of an *in vitro* assay for chemical carcinogenesis testing. CTA has demonstrated to be a powerful tool in the study of carcinogenesis since it mimics *in vitro* the different phases of *in vivo* initiation, promotion/progression and tumor formation (OECD, 2007). These assays are suggested as part of the Integrated Approaches to Testing and Assessment (IATA) in which the CTA is a possible building block within the carcinogenesis study and not a stand-alone assay (Corvi et al., 2017). Within this vision and approach, we have initially applied the CTA to the identification of cadmium-induced *in vitro* carcinogenesis (Forcella et al., 2016) and subsequently to the comprehension and identification of markers and hallmarks of transformed cells (Oldani et al., 2021). Finally, in this work, transcriptomics represented a powerful tool to identify early molecular markers of carcinogenesis and improve CTA, as previously proposed (Colacci et al., 2023; Mascolo et al., 2018), and allowed to confirm mitochondria as early targets of cadmium toxicity, even at sublethal concentrations; moreover, ribosomes and the cytoskeleton were also identified as cadmium targets and will be further investigated in the future. Transcriptomics and epigenetic mechanisms, which are largely to be explored, along with protein expression analysis and morphological and metabolic assessment, could therefore lead to a comprehensive understanding of Cd-induced carcinogenesis.

CRediT authorship contribution statement

Monica Oldani: Writing – review & editing, Writing – original draft, Visualization, Methodology, Investigation, Formal analysis, Data curation. **Marco Fabbri:** Writing – review & editing, Writing – original draft, Visualization, Methodology, Investigation, Formal analysis, Data curation. **Pasquale Mechioretto:** Writing – review & editing, Investigation. **Matilde Forcella:** Writing – review & editing, Writing – original draft, Validation, Supervision, Project administration, Conceptualization. **Paola Fusi:** Writing – review & editing, Writing – original draft, Supervision, Resources, Funding acquisition, Conceptualization. **Chiara Urani:** Writing – review & editing, Writing – original draft, Supervision, Resources, Funding acquisition, Conceptualization.

Funding

This work was supported by the University of Milano-Bicocca (2023-ATE-0271 to PF and 2023-ATE-0523 to CU)

Declaration of competing interest

The authors declare that they have no known competing financial interests or personal relationships that could have appeared to influence the work reported in this paper.

Appendix A. Supplementary data

Supplementary data to this article can be found online at https://doi.org/10.1016/j.fct.2026.116492.

Data availability

I have shared the link to my data in the manuscript: https://www.ncbi.nlm.nih.gov/geo/query/acc.cgi?acc=GSE328009.

References

Asara, Y., Marchal, J.A., Carrasco, E., Boulaiz, H., Solinas, G., Bandiera, P., Garcia, M.A., Farace, C., Montella, A., Madeddu, R., 2013. Cadmium modifies the cell cycle and apoptotic profiles of human breast cancer cells treated with 5-fluorouracil. Int. J. Mol. Sci. 14, 16600–16616. https://doi.org/10.3390/ijms140816600.

Bernard, A., 2008. Cadmium & its adverse effects on human health. Indian J. Med. Res. 128.

Bertin, G., Averbeck, D., 2006. Cadmium: cellular effects, modifications of biomolecules, modulation of DNA repair and genotoxic consequences (a review). Biochimie 88, 1549–1559. https://doi.org/10.1016/J.BIOCHI.2006.10.001.

Binder, M.J., McCoombe, S., Williams, E.D., McCulloch, D.R., Ward, A.C., 2020. ADAMTS-15 has a tumor suppressor role in prostate cancer. Biomolecules 10, 682. https://doi.org/10.3390/biom10050682.

Bovio, F., Ferrian, M., Franceschi, A., Melchioretto, P., Porru, S., Forcella, M., Fusi, P., Urani, C., 2026. Cadmium accumulation in neuronal cells leads to essential metals imbalance and zinc transporters dysregulation. Toxicology 519, 154319. https://doi.org/10.1016/j.tox.2025.154319.

Bovio, F., Melchioretto, P., Forcella, M., Fusi, P., Urani, C., 2021. Cadmium promotes glycolysis upregulation and glutamine dependency in human neuronal cells. Neurochem. Int. 149, 105144. https://doi.org/10.1016/J.NEUINT.2021.105144.

Bovio, F., Perciballi, E., Melchioretto, P., Ferrari, D., Forcella, M., Fusi, P., Urani, C., 2024. Morphological and metabolic changes in microglia exposed to cadmium: cues on neurotoxic mechanisms. Environ. Res. 240, 117470. https://doi.org/10.1016/j.envres.2023.117470.

Branca, J.J.V., Pacini, A., Gulisano, M., Taddei, N., Fiorillo, C., Becatti, M., 2020. Cadmium-Induced cytotoxicity: effects on mitochondrial electron transport chain. Front. Cell Dev. Biol. 8.

Callegaro, G., Forcella, M., Melchioretto, P., Frattini, A., Gribaldo, L., Fusi, P., Fabbri, M., Urani, C., 2018. Toxicogenomics applied to in vitro cell transformation Assay reveals mechanisms of early response to cadmium. Toxicol. Vitro 48, 232–243. https://doi.org/10.1016/J.TIV.2018.01.025.

Cirovic, A., Satarug, S., 2024. Toxicity tolerance in the carcinogenesis of environmental cadmium. Int. J. Mol. Sci. https://doi.org/10.3390/ijms25031851.

Cirovic, Ana, Cirovic, Aleksandar, Yimthiang, S., Vesey, D.A., Satarug, S., 2024. Modulation of adverse health effects of environmental cadmium exposure by zinc and its transporters. Biomolecules 14, 650. https://doi.org/10.3390/biom14060650.

Colacci, A., Corvi, R., Ohmori, K., Paparella, M., Serra, S., Da Rocha Carrico, I., Vasseur, P., Jacobs, M.N., 2023. The cell transformation assay: a historical assessment of current knowledge of applications in an integrated approach to testing and assessment for non-genotoxic carcinogens. Int. J. Mol. Sci. 24, 5659. https://doi.org/10.3390/ijms24065659.

Conway, J.R., Lex, A., Gehlenborg, N., 2017. UpSetR: an R package for the visualization of intersecting sets and their properties. Bioinformatics 33, 2938–2940. https://doi.org/10.1093/bioinformatics/btx364.

Corvi, R., Madia, F., Guyton, K.Z., Kasper, P., Rudel, R., Colacci, A., Kleinjans, J., Jennings, P., 2017. Moving forward in carcinogenicity assessment: report of an EURL ECVAM/ESTIV workshop. Toxicol. Vitro 45, 278–286. https://doi.org/10.1016/J.TIV.2017.09.010.

Cox, T.R., Erler, J.T., 2011. Remodeling and homeostasis of the extracellular matrix: implications for fibrotic diseases and cancer. Dis. Model. Mech. 4, 165–178. https://doi.org/10.1242/dmm.004077.

Dunn, J.R., Reed, J.E., du Plessis, D.G., Shaw, E.J., Reeves, P., Gee, A.L., Warnke, P., Walker, C., 2006. Expression of ADAMTS-8, a secreted protease with antiangiogenic properties, is downregulated in brain tumours. Br. J. Cancer 94, 1186–1193. https://doi.org/10.1038/sj.bjc.6603006.

Fabbri, M., Urani, C., Sacco, M.G., Procaccianti, C., Gribaldo, L., 2012. Whole genome analysis and microRNAs regulation in HepG2 cells exposed to cadmium. ALTEX - Altern. Anim. Experim. 29, 173–182. https://doi.org/10.14573/altex.2012.2.173.

Fang, M., Yuan, J., Peng, C., Li, Y., 2014. Collagen as a double-edged sword in tumor progression. Tumor Biol. 35, 2871–2882. https://doi.org/10.1007/s13277-013-1511-7.

Fares, J., Fares, M.Y., Khachfe, H.H., Salhab, H.A., Fares, Y., 2020. Molecular principles of metastasis: a hallmark of cancer revisited. Signal Transduct. Targeted Ther. 5, 28. https://doi.org/10.1038/s41392-020-0134-x.

Forcella, M., Callegaro, G., Melchioretto, P., Gribaldo, L., Frattini, M., Stefanini, F.M., Fusi, P., Urani, C., 2016. Cadmium-transformed cells in the in vitro cell transformation assay reveal different proliferative behaviours and activated pathways. Toxicol. Vitro 36, 71–80. https://doi.org/10.1016/J.TIV.2016.07.006.

Forcella, M., Lau, P., Fabbri, M., Fusi, P., Oldani, M., Melchioretto, P., Gribaldo, L., Urani, C., 2022. Is cadmium toxicity tissue-specific? Toxicogenomics studies reveal common and specific pathways in pulmonary, hepatic, and neuronal cell models. Int. J. Mol. Sci. 23. https://doi.org/10.3390/ijms23031768.

Forcella, M., Lau, P., Oldani, M., Melchioretto, P., Bogni, A., Gribaldo, L., Fusi, P., Urani, C., 2020. Neuronal specific and non-specific responses to cadmium possibly involved in neurodegeneration: a toxicogenomics study in a human neuronal cell model. Neurotoxicology 76, 162–173. https://doi.org/10.1016/J.NEURO.2019.11.002.

Fuentes, P., Pelletier, J., Gentilella, A., 2024. Decoding ribosome complexity: role of ribosomal proteins in cancer and disease. NAR Cancer 6. https://doi.org/10.1093/narcan/zcae032.

Ge, S.X., Jung, D., Yao, R., 2020. ShinyGO: a graphical gene-set enrichment tool for animals and plants. Bioinformatics 36, 2628–2629. https://doi.org/10.1093/bioinformatics/btz931.

Gentleman, R.C., Carey, V.J., Bates, D.M., Bolstad, B., Dettling, M., Dudoit, S., Ellis, B., Gautier, L., Ge, Y., Gentry, J., Hornik, K., Hothorn, T., Huber, W., Iacus, S., Irizarry, R., Leisch, F., Li, C., Maechler, M., Rossini, A.J., Sawitzki, G., Smith, C., Smyth, G., Tierney, L., Yang, J.Y.H., Zhang, J., 2004. Bioconductor: open software development for computational biology and bioinformatics. Genome Biol. 5, R80. https://doi.org/10.1186/gb-2004-5-10-r80.

Henkler, F., Brinkmann, J., Luch, A., 2010. The role of oxidative stress in carcinogenesis induced by metals and xenobiotics. Cancers (Basel). https://doi.org/10.3390/cancers2020376.

Jaishankar, M., Tseten, T., Anbalagan, N., Mathew, B.B., Beeregowda, K.N., 2014. Toxicity, mechanism and health effects of some heavy metals. Interdiscip. Toxicol. https://doi.org/10.2478/intox-2014-0009.

Kato, H., Mihara, K., 2008. Identification of Tom5 and Tom6 in the preprotein translocase complex of human mitochondrial outer membrane. Biochem. Biophys. Res. Commun. 369, 958–963. https://doi.org/10.1016/J.BBRC.2008.02.150.

Kim, D.J., 2026. Molecular and immune mechanisms governing cancer metastasis, including dormancy, microenvironmental niches, and tumor-specific programs. Int. J. Mol. Sci. 27, 875. https://doi.org/10.3390/ijms27020875.

Koizumi, S., Yamada, H., 2003. DNA microarray analysis of altered gene expression in cadmium-exposed human cells. J. Occup. Health 45, 331–334. https://doi.org/10.1539/joh.45.331.

Komiya, T., Rospert, S., Koehler, C., Looser, R., Schatz, G., Mihara, K., 1998. Interaction of mitochondrial targeting signals with acidic receptor domains along the protein import pathway: evidence for the 'acid chain' hypothesis. EMBO J. 17, 3886–3898. https://doi.org/10.1093/emboj/17.14.3886.

Laemmli, U.K., 1970. Cleavage of structural proteins during the assembly of the head of bacteriophage T4. Nature 227, 680–685.

Langfelder, P., Horvath, S., 2008. WGCNA: an R package for weighted correlation network analysis. BMC Bioinf. 9, 559. https://doi.org/10.1186/1471-2105-9-559.

Lee, W.-K., Thévenod, F., 2020. Cell organelles as targets of mammalian cadmium toxicity. Arch. Toxicol. 94, 1017–1049. https://doi.org/10.1007/s00204-020-02692-8.

Levental, K.R., Yu, H., Kass, L., Lakins, J.N., Egeblad, M., Erler, J.T., Fong, S.F.T., Csiszar, K., Giaccia, A., Weninger, W., Yamauchi, M., Gasser, D.L., Weaver, V.M., 2009. Matrix crosslinking forces tumor progression by enhancing Integrin signaling. Cell 139, 891–906. https://doi.org/10.1016/j.cell.2009.10.027.

Liu, Z., Huang, R., Roberts, R., Tong, W., 2019. Toxicogenomics: a 2020 vision. Trends Pharmacol. Sci. https://doi.org/10.1016/j.tips.2018.12.001.

Llamazares, M., Obaya, A.J., Moncada-Pazos, A., Heljasvaara, R., Espada, J., López-Otín, C., Cal, S., 2007. The ADAMTS12 metalloproteinase exhibits anti-tumorigenic properties through modulation of the Ras-dependent ERK signalling pathway. J. Cell Sci. 120, 3544–3552. https://doi.org/10.1242/jcs.005751.

Luparello, C., 2021. Cadmium-associated molecular signatures in cancer cell models. Cancers (Basel) 13, 2823. https://doi.org/10.3390/cancers13112823.

Mascolo, M.G., Perdichizzi, S., Vaccari, M., Rotondo, F., Zanzi, C., Grilli, S., Paparella, M., Jacobs, M.N., Colacci, A., 2018. The transformics assay: first steps for the development of an integrated approach to investigate the malignant cell transformation in vitro. Carcinogenesis 39, 955–967. https://doi.org/10.1093/carcin/bgy037.

Mezynska, M., Brzóska, M., 2018. Environmental exposure to cadmium—a risk for health of the general population in industrialized countries and preventive strategies. Environ. Sci. Pollut. Res. 25. https://doi.org/10.1007/s11356-017-0827-z.

Nilusha, R., Julien, D., Elodie, S., Florent, B., Christophe, N., Nathalie, J., Jean-Marie, D., Fernando, R.-L., 2010. Cadmium alters the biotransformation of carcinogenic aromatic amines by arylamine N-Acetyltransferase xenobiotic-metabolizing enzymes: molecular, cellular, and in vivo studies. Environ. Health Perspect. 118, 1685–1691. https://doi.org/10.1289/ehp.1002334.

OECD, 2007. Detailed review paper on cell transformation assays for detection of chemical carcinogens, OECD environment, health and Safety Publications. Series on Testing and Assessment No. 31, p. 18.

Oldani, M., Manzoni, M., Villa, A.M., Stefanini, F.M., Melchioretto, P., Monti, E., Forcella, M., Urani, C., Fusi, P., 2020b. Cadmium elicits alterations in mitochondrial morphology and functionality in C3H10T1/2Cl8 mouse embryonic fibroblasts. Biochim. Biophys. Acta Gen. Subj. 1864, 129568. https://doi.org/10.1016/j.bbagen.2020.129568.

Oldani, M., Villa, A.M., Manzoni, M., Melchioretto, P., Parenti, P., Monti, E., Fusi, P., Forcella, M., Urani, C., 2021. Insights into cadmium-induced carcinogenesis through an In vitro study using C3H10T1/2Cl8 cells: the multifaceted role of mitochondria. Int. J. Mol. Sci. 22, 10837. https://doi.org/10.3390/ijms221910837.

Oldani, Monica, Fabbri, M., Melchioretto, P., Callegaro, G., Fusi, P., Gribaldo, L., Forcella, M., Urani, C., 2020a. In vitro and bioinformatics mechanistic-based approach for cadmium carcinogenicity understanding. Toxicol. Vitro 65, 104757. https://doi.org/10.1016/J.TIV.2020.104757.

Orth, M.F., Hölting, T.L.B., Dallmayer, M., Wehweck, F.S., Paul, T., Musa, J., Baldauf, M. C., Surdez, D., Delattre, O., Knott, M.M.L., Romero-Pérez, L., Kasan, M., Cidre-Aranaz, F., Gerke, J.S., Ohmura, S., Li, J., Marchetto, A., Henssen, A.G., Özen, Ö., Sugita, S., Hasegawa, T., Kanaseki, T., Bertram, S., Dirksen, U., Hartmann, W., Kirchner, T., Grünewald, T.G.P., 2020. High specificity of BCL11B and GLG1 for EWSR1-fli1 and EWSR1-ERG positive Ewing sarcoma. Cancers (Basel) 12. https://doi.org/10.3390/cancers12030644.

Osaki, M., Oshimura, M., Ito, H., 2004. PI3K-Akt pathway: its functions and alterations in human cancer. Apoptosis 9, 667–676. https://doi.org/10.1023/B:APPT.0000045801.15585.dd.

Peana, M., Pelucelli, A., Chasapis, C.T., Perlepes, S.P., Bekiari, V., Medici, S., Zoroddu, M. A., 2022. Biological effects of human exposure to environmental cadmium. Biomolecules 13, 36. https://doi.org/10.3390/biom13010036.

Petering, D.H., 2017. Reactions of the Zn proteome with Cd2+ and other xenobiotics: trafficking and toxicity. Chem. Res. Toxicol. 30, 189–202. https://doi.org/10.1021/acs.chemrestox.6b00328.

Piao, X.-M., Hwang, B., Jeong, P., Byun, Y., Kang, H., Seo, S., Kim, W., Lee, J.-Y., Ha, Y.-S., Lee, Y.-S., Kim, I., Choi, Y., Cha, E.-J., Moon, S.-K., Yun, S., Kim, W.-J., 2021. Collagen type VI-α1 and 2 repress the proliferation, migration and invasion of bladder cancer cells. Int. J. Oncol. 59, 37. https://doi.org/10.3892/ijo.2021.5217.

Pitt, A.S., Buchanan, S.K., 2021. A biochemical and structural understanding of tom complex interactions and implications for human health and disease. Cells 10. https://doi.org/10.3390/cells10051164.

Qu, F., Zheng, W., 2024. Cadmium exposure: mechanisms and pathways of toxicity and implications for human health. Toxics 12, 388. https://doi.org/10.3390/toxics12060388.

Ramkumar, N., Baum, B., 2016. Coupling changes in cell shape to chromosome segregation. Nat. Rev. Mol. Cell Biol. 17, 511–521. https://doi.org/10.1038/nrm.2016.75.

Rasin, P., V, A.A., Basheer, S.M., Haribabu, J., Santibanez, J.F., Garrote, C.A., Arulraj, A., Mangalaraja, R.V., 2025. Exposure to cadmium and its impacts on human health: a short review. J. Hazard. Mater. Adv. 17, 100608. https://doi.org/10.1016/j.hazadv.2025.100608.

Ritchie, M.E., Phipson, B., Wu, D., Hu, Y., Law, C.W., Shi, W., Smyth, G.K., 2015. Limma powers differential expression analyses for RNA-sequencing and microarray studies. Nucleic Acids Res. 43. https://doi.org/10.1093/nar/gkv007 e47–e47.

Ronco, A.M., Llaguno, E., Epuñan, M.J., Llanos, M.N., 2010. Effect of cadmium on cortisol production and 11β-hydroxysteroid dehydrogenase 2 expression by cultured human choriocarcinoma cells (JEG-3). Toxicol. Vitro 24, 1532–1537. https://doi.org/10.1016/J.TIV.2010.07.003.

Ryoo, S.-W., Choi, B.-Y., Son, S.-Y., Lee, J.-H., Min, J.-Y., Min, K.-B., 2025. Lead and cadmium exposure was associated with faster epigenetic aging in a representative sample of adults aged 50 and older in the United States. Chemosphere 374, 144194. https://doi.org/10.1016/j.chemosphere.2025.144194.

Schauder, A., Avital, A., Malik, Z., 2010. Regulation and gene expression of heme synthesis under heavy metal exposure-review. J. Environ. Pathol. Toxicol. Oncol. 29.

Smith, P.K., Krohn, R.I., Hermanson, G.T., Mallia, A.K., Gartner, F.H., Provenzano, M.D., Fujimoto, E.K., Goeke, N.M., Olson, B.J., Klenk, D.C., 1985. Measurement of protein using bicinchoninic acid. Anal. Biochem. 150, 76–85. https://doi.org/10.1016/0003-2697(85)90442-7.

Smyth, G.K., 2004. Linear models and empirical bayes methods for assessing differential expression in microarray experiments. Stat. Appl. Genet. Mol. Biol. 3. https://doi.org/10.2202/1544-6115.1027.

Tan, H.W., Seen, D.L.T., Xu, Y.-M., Lau, A.T.Y., 2023. Cadmium, cellular senescence. Cancer. Rev. Environ. Contam. Toxicol. 261, 21. https://doi.org/10.1007/s44169-023-00042-0.

Thévenod, F., Lee, W.-K., 2013. Toxicology of cadmium and its damage to mammalian organs. Cadmium: Toxicit. Essent. 415–490.

Urani, C., Stefanini, F.M., Bussinelli, L., Melchiretto, P., Crosta, G.F., 2009. Image analysis and automatic classification of transformed foci. J. Microsc. 234, 269–279. https://doi.org/10.1111/j.1365-2818.2009.03171.x.

Vázquez, F., Hastings, G., Ortega, M.A., Lane, T.F., Oikemus, S., Lombardo, M., Iruela-Arispe, M.L., 1999. METH-1, a human ortholog of ADAMTS-1, and METH-2 are members of a new family of proteins with angio-inhibitory activity. J. Biol. Chem. 274, 23349–23357. https://doi.org/10.1074/jbc.274.33.23349.

Viloria, C.G., Obaya, A.J., Moncada-Pazos, A., Llamazares, M., Astudillo, A., Capellá, G., Cal, S., López-Otín, C., 2009. Genetic inactivation of ADAMTS15 metalloprotease in human colorectal cancer. Cancer Res. 69, 4926–4934. https://doi.org/10.1158/0008-5472.CAN-08-4155.

Wisdom, R., Johnson, R.S., Moore, C., 1999. c-Jun regulates cell cycle progression and apoptosis by distinct mechanisms. EMBO J. 18, 188–197. https://doi.org/10.1093/emboj/18.1.188.

Wuana, R.A., Okieimen, F.E., 2011. Heavy metals in contaminated soils: a review of sources, chemistry, risks and best available strategies for remediation. Int. Sch. Res. Not. 2011, 402647. https://doi.org/10.5402/2011/402647.

Xu, G., Li, T., Chen, J., Li, C., Zhao, H., Yao, C., Dong, H., Wen, K., Wang, K., Zhao, J., Xia, Q., Zhou, T., Zhang, H., Gao, P., Li, A., Pan, X., 2018. Autosomal dominant retinitis pigmentosa-associated gene PRPF8 is essential for hypoxia-induced mitophagy through regulating ULK1 mRNA splicing. Autophagy 14, 1818–1830. https://doi.org/10.1080/15548627.2018.1501251.

Yang, H., Shu, Y., 2015. Cadmium transporters in the kidney and cadmium-induced nephrotoxicity. Int. J. Mol. Sci. https://doi.org/10.3390/ijms16011484.

Yang, Y., Hassan, M.F., Ali, W., Zou, H., Liu, Z., Ma, Y., 2025. Effects of cadmium pollution on human health: a narrative review. Atmosphere (Basel) 16, 225. https://doi.org/10.3390/atmos16020225.

Zhao, L., Islam, R., Wang, Y., Zhang, X., Liu, L.-Z., 2022. Epigenetic regulation in Chromium-, Nickel- and cadmium-induced carcinogenesis. Cancers (Basel) 14, 5768. https://doi.org/10.3390/cancers14235768.

Zhou, T., Jia, X., Chapin, R.E., Maronpot, R.R., Harris, M.W., Liu, J., Waalkes, M.P., Eddy, E.M., 2004. Cadmium at a non-toxic dose alters gene expression in mouse testes. Toxicol. Lett. 154, 191–200. https://doi.org/10.1016/J.TOXLET.2004.07.015.

Zhu, Y., Costa, M., 2020. Metals and molecular carcinogenesis. Carcinogenesis 41, 1161–1172. https://doi.org/10.1093/carcin/bgaa076.